

Aggregate structure of “single-nano buckydiamond” in gel and dried powder by differential scanning calorimetry and nitrogen adsorption

Mikhail V. Korobov^{a,*}, Maria M. Batuk^b, Natalia V. Avramenko^a, Nina I. Ivanova^a,
Natalia N. Rozhkova^c, Eiji Ōsawa^d

^a Department of Chemistry, Moscow State University, Moscow 119899, Russia

^b Department of Materials Science, Moscow State University, Moscow 119899, Russia

^c Institute of Geology, Karelian Research Centre RAS, Petrozavodsk, Russia

^d NanoCarbon Research Institute, AREC, Faculty of Textile Science and Engineering, Shinshu University, 3-15-1 Tokita, Ueda 386-8567, Japan

ARTICLE INFO

Article history:

Received 27 July 2009

Received in revised form 23 January 2010

Accepted 17 February 2010

Available online 24 February 2010

Keywords:

Detonation nanodiamond

Primary particles

Differential scanning calorimetry

Nitrogen adsorption

Mesoporous secondary structure

ABSTRACT

Gels and dried powders of the single-nano buckydiamond (SNBD) have been studied by means of differential scanning calorimetry (DSC) and gas adsorption methods. Nanophase of water (NPhW) was confirmed in SNBD hydrogel by DSC, wherein the characteristic feature at 265 K was observed and attributed to melting of NPhW. No such feature was observed in commercial agglutinate samples of detonation nanodiamond. The parameters of the DSC peak were independent on the method of the material preparation and reproducible to serve as a fingerprint of SNBD material itself. The same nanophase was found in dried powders of SNBD after they were equilibrated with water vapor in isopiestic experiments. Nitrogen adsorption isotherms of the dried powder demonstrated the presence of nano voids. The characteristic size and volume of the nano voids were almost equal to those of NPhW. Gels and dried powders were easily converted back into SNBD water dispersions. Based on DSC and adsorption data it was concluded that SNBD material, though originally divided into individual diamond crystals ($d = 5.2$ nm) in the water dispersion, forms stable porous networks as gel and dried powder. Formation of such networks could be explained in terms of Van der Waals or Coulombic interaction between the SNBD particles.

© 2010 Elsevier B.V. All rights reserved.

1. Introduction

Detonation nanodiamond (ND) is a unique carbon material with potential applications in nanotechnology [1]. The crude product isolated from detonation soot consists of tight agglomerate particles having 100–200 nm in diameter, called *agglutinates*. Applications of agglutinates are described in Ref. [2–7]. The structure and composition of agglutinates are well discussed in the literature [1,8–15]. An agglutinate is composed of primary particles (diameter 4–5 nm, *single-nano buckydiamond, SNBD*) of detonation ND, which in turn have triple core-shell structure with sp^2 graphitic layers surrounding $sp^{2+x} + sp^3$ diamond core. The shell is probably more correctly described as holey giant fullerene. The presence of sp^2 carbon in cleaned primary particles was not confirmed recently by careful ^{13}C NMR measurements [15]. It was often thought that in agglutinate the primary SNBD particles are bound by multitudes of C–C covalent bonds with neighboring particles [1]. Recently Barnard [8,9] showed that agglutination could be due to coherent Coulombic interparticle bonding between the facets having opposite signs. According to her

DFTB calculations, if the facet–facet orientation is coherent the Coulombic energy between SNBDs at proper separation approaches the C–C bond energy. Calculations were performed on polyhedra as models of SNBD particles. Chemically clean facets were also implicit [9].

One of us has succeeded in disintegrating the agglutinates into SNBD particles by means of stirred-media milling in water to give surprisingly time-stable aqueous colloidal dispersion [11]. Sharp particle-size distribution of SNBD was confirmed in these dispersions by means of dynamic light scattering (DLS), small-angle X-ray diffraction and HRTEM measurements. In the optimized condition of milling, 10 wt.% suspension of commercial gray fine powder of agglutinates is processed to give a black colloidal solution with the same concentration in quantitative yield. At this concentration, sometimes the colloidal solution turns into very soft and black hydrogel upon standing a few days. Removal of water from the soft gel in a rotary evaporator leads to harder and harder gels and flakes, finally to dry powder, dark brown to black depending on the size of conglomerates. Gel and dried powder are re-dispersible.

Preparation and properties of SNBD material were discussed in [1,11]. In Ref. [11] the authors among other things described the purification procedure. Infra Red spectra of the chemical groups on SNBD surfaces were given in [1,11].

* Corresponding author. Fax: +7 495 9328846.

E-mail address: mkorobov49@gmail.com (M.V. Korobov).

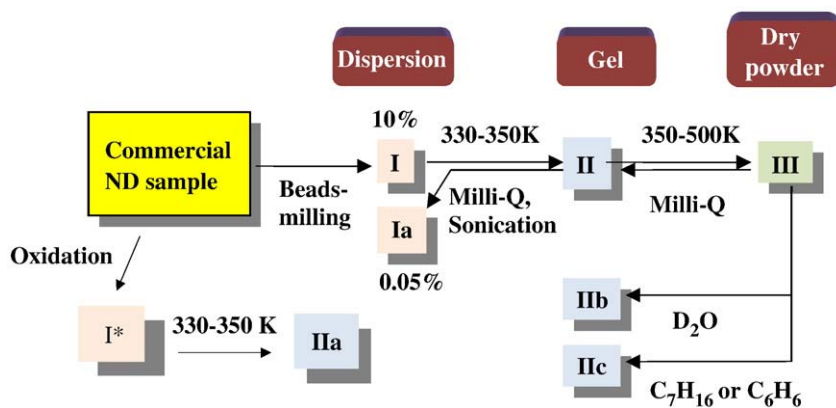


Fig. 1. Interrelation among SNBD samples (I–III) prepared in this work.

SNBD gels were examined by means of DSC, which demonstrated the presence of Nanophase of Water (NPhW) [16]. STEM images of the dried SNBD powders were reported by Yakubovskii et al. [17]. All these three forms of SNBD material have found different applications, but the most intriguing among them is gel, which recently found to become a potentially useful platform for drug carrier for cancer therapy [18–20]. However, the mode of action between the SNBD platform and anti-cancer drug molecules like doxorubicin remained unclear. An alternative method of disintegration of agglutinates was reported recently by Gubarevich and her group [14]. This method is based on catalytic oxidation of the agglutinates. The presence of the primary particles in the resulting dispersion was proved by DLS.

The goal of this study is to gain more insight into the nature of the SNBD hydrogel and dried powder. DSC and combined isopiestic equilibrium hydration with DSC were used to study gel. Using DSC for such type of measurements is not routine, however, examples may be found in the literature [21–26] and even for nanomaterials [25] and gels of nanomaterials [26]. Dried powders were examined by means of gas adsorption, a technique typically used to detect mesopores in bulk materials. We obtained reproducible structural parameters of gel and dry powder of SNBD. These parameters are the size and the volume of voids formed.

2. Experimental

Commercial detonation nanodiamond, produced by Gansu Goldstone Nano-Material Co., Ltd., Lanzhou, China, was used as the starting material. The powder product was the mixed conglomerates showing discrete size distribution between 200 nm and 20 μm . This powder was suspended in excess water and subjected to stirred-media milling with zirconia beads having an average diameter of 30 μm to give a clear colloidal solution of disintegrated primary SNBD particles (I). The preparation of aqueous SNBD colloidal solution I was described in detail elsewhere [11]. Two other forms of SNBD were prepared from I by removing water under nitrogen or air. Gel samples (II) with the mass ratio of SNBD to water above 1:10 were made by evaporating water from colloidal solution at 330–350 K. Dry powder (III) was produced from I or II by complete removal of water at 350–500 K. Elemental analysis of III performed using Carbo-Erbo Mode-1106 instrument yielded C/H/N ratios of 100(91.4 wt.)/2.40/1.05. Infra Red spectra of chemical groups on the surface of III were recorded on Magna-IR 750 (Nicolet) FTIR spectrometer. IR signals (cm^{-1}) detected were 3380 (ν_{OH}), 2920 (ν_{CH}), 1719 (ν_{CO}), and 1625 (δ_{OH}). IR spectrum was similar to the one reported in Ref. [1] for original SNBD material. It is typical to ND materials in contact with the air. Gel II was also produced from III by addition of Milli-Q water followed by simple mixing/ultrasonication. It was possible to turn samples II into III and back several times. The measured properties of samples studied

here did not change throughout these treatments (see below). We had in our disposal one sample (I*) of aqueous SNBD colloidal solution prepared according to the “wet” procedure described in Ref. [14].¹ This sample was turned into the gel sample (IIa) by evaporating of water.

Gel in D₂O (IIb) was prepared from III by addition of D₂O instead of H₂O. Nonaqueous gel (IIc) was obtained from III by addition of benzene or heptane. Transparent colloidal solutions of SNBD (Ia) in water with the concentrations ~0.5 mg/ml were prepared from II or III by addition of the Milli-Q water followed by mild sonication (20–80 W, 30 min) in ultrasonic bath. Preparation of the samples is illustrated in Fig. 1.

Gel samples II, IIa, IIb and IIc were studied by DSC on a DSC-30 TA from Mettler and DSC-204 F1 from Netzsch Instruments to capture the heating traces from 173 up to 323 K. The scanning rates were 10, 5, and 2 K/min. The DSC experimental procedure is described in detail elsewhere [16]. Typically 10 mg of SNBD material was used in one experiment. The minimum amount of SNBD necessary for one run was 1 mg. The suitable mass ratio of SNBD to water (or organic solvent) in the sample is 1:1.

Samples II and III were equilibrated with water under the isopiestic condition. A sample was placed into a closed chamber ($T = 298 \text{ K}$) along with the saturated aqueous solutions of KNO₃ ($p/p^0 = 0.9$) for two weeks. Samples III are saturated with water through the vapor phase, while samples II lost some water during equilibration. After the equilibrium was reached, the DSC traces of the samples were taken according to the procedure described above.

Nitrogen absorption measurements were carried out on the dry powder sample III using Micrometrics ASAP 2010 apparatus. Particle-size distributions in dilute aqueous dispersions of SNBD, Ia, were measured by means of dynamic light scattering (DLS) method using Malvern Zetasizer nanoZS instrument. TEM images were recorded with a LE0912 AB OMEGA instrument ($E = 120 \text{ kV}$).

3. Results

3.1. DSC traces of the gel samples, II, IIa and IIb

Two endothermic peaks appeared near 273 K in the DSC heating traces of gel sample II. The typical heating trace is presented in Fig. 2 along with the heating trace of the “gel” prepared from the commercial material before stirred-media milling.

The feature at $273.2 \pm 0.5 \text{ K}$ corresponds obviously to the melting of bulk water. An additional broad endothermic feature was observed at temperatures below $T = 273 \text{ K}$ for sample II. The appearance of the

¹ We are grateful to the authors of Ref. [14] who distributed such samples among the participants of the 3rd International Symposium “Detonation Nanodiamonds: Technology, Properties and Applications” in S. Petersburg (2008) for free.

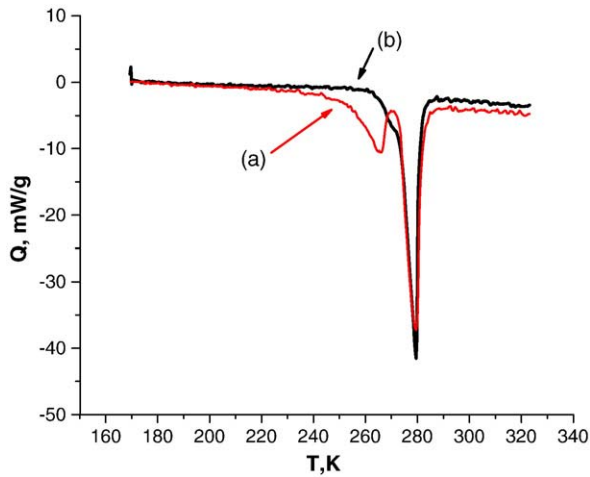


Fig. 2. DSC traces of nanodiamond gels: (a) SNBD gel, II; (b) “Gel” prepared from “commercial diamond nanoparticles”(agglutinates). The amounts of nanodiamond and the nanodiamond-to-H₂O mass ratio are the same in both samples.

broad peak is a result of the milling procedure [11] as it is absent in the heating trace for the “gels” of the commercial material. The samples of different commercial materials were examined. The features at $T=273$ K had different shapes, but the peak at $T=265$ K was never observed. More than 50 samples of II were studied to obtain the average difference between the two peak maxima, ΔT_m , of 8.3 ± 0.5 K.

When water was replaced by D₂O both peaks were shifted towards higher temperature by almost 4 K (Fig. 3). This shift is equal to the difference between the melting temperatures of H₂O and D₂O.

Based on these observations we conclude that the broad peak at $T=265 \pm 0.5$ K for SNBD hydrogel corresponds to the phase transformation in water, namely it was assigned to the melting of nanophase of H₂O (NPhW). The dependence of the melting temperature on the diameter, D , of the phase is accounted for by Gibbs–Kelvin equation,

$$\Delta T_m = \frac{4\sigma_{s-l}V_L T_m}{D\Delta H_m} \quad (1)$$

where σ_{s-l} is the surface tension of the solid–liquid interface [22], V_L , T_m , ΔH_m are the molar volume of liquid, the melting point and the enthalpy of melting of bulk water, respectively [27], and $\Delta T_m = T_m - T$ is the size-dependent depression of melting point, determined directly from the DSC curves.

Measured $\Delta T_m = 8.3 \pm 0.5$ K corresponds to characteristic diameter of NPhW equal to 8.0 ± 1.0 nm.

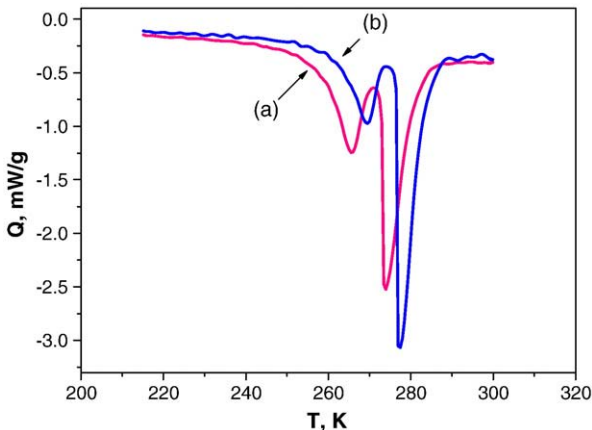


Fig. 3. DSC traces of the ND gels. (a) H₂O gel; (b) D₂O gel.

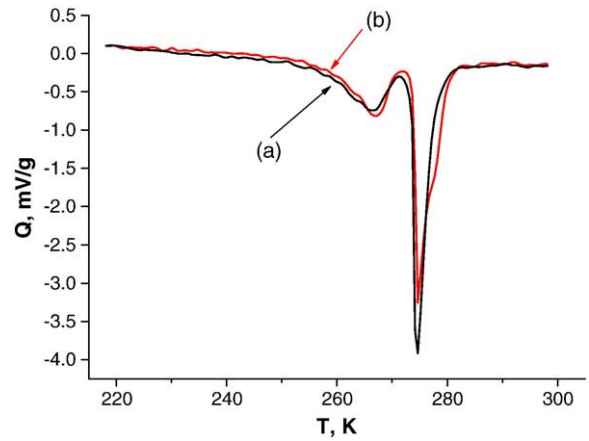


Fig. 4. DSC traces of nanodiamond gels: (a) SNBD gel, II; (b) SNBD gel, IIa.

Efforts were made in order to see if the characteristic size of NPhW will change or not:

- Gel samples II were prepared from sample I or from sample III (see Experimental).
- Powder samples III were pressed into tablets under the pressure of 70 bar and/or annealed at $T=700$ K prior to addition of Milli-Q water to the prepared DSC samples.

However, the depression of freezing temperature ΔT_m (8.3 ± 0.5 K) was independent on the way of preparation and the pretreatment conditions described above.

The heating traces for samples II and IIa are compared in Fig. 4. The traces are almost identical, though disintegration procedures in Ref. [14] and in the present study were different.

One can assume that ΔT_m is a stable characteristic of the hydrogel samples of SNBD.

In addition to ΔT_m , two other independent parameters of NPhW were obtained from the DSC traces, namely the total volume of the NPhW in the sample, $V_{H_2O, nm}$, and the volume of freezing NPhW, $V_{H_2O, nm, f}$. Both values were referred to the unit mass of SNBD in the sample. $V_{H_2O, nm}$ was calculated using the following equations:

$$M_{H_2O, b} = Q_{273K} / \Delta H_m$$

$$M_{H_2O, nm} = M_{H_2O} - M_{H_2O, b} = M_{H_2O} - Q_{273K} / \Delta H_m \quad (2)$$

$$V_{H_2O, nm} = \frac{M_{H_2O, nm}}{\rho_{H_2O}}$$

where M_{H_2O} , $M_{H_2O, b}$, and $M_{H_2O, nm}$ denote total mass of water determined by weighing, mass of a bulk water and mass of a non-bulk water in the sample, respectively; Q_{273K} denotes the DSC-measured enthalpy that corresponds to the endothermic feature at 273 K, ΔH_m and ρ_{H_2O} are the standard enthalpy of melting and density at $T=273$ K of bulk water, respectively [27].

For bulk porous materials it is usually assumed that part of NPhW does not participate itself in the melting/freezing process. In our case this non-freezing fraction covers the surface of SNBD. The enthalpy of melting for the rest part of the NPhW is the same as for the bulk [22–24]. The amounts of freezing NPhW, $M_{H_2O, nm, f}$, and of non-freezing NPhW, $M_{H_2O, nm, nf}$ were determined from the DSC data:

$$M_{H_2O, nm, f} = \frac{Q_{265}}{\Delta H_m}; \quad M_{H_2O, nm, nf} = M_{H_2O, nm} - M_{H_2O, nm, f} \quad (3)$$

$$V_{H_2O, nm, f} = \frac{M_{H_2O, nm, f}}{\rho_{H_2O}}$$

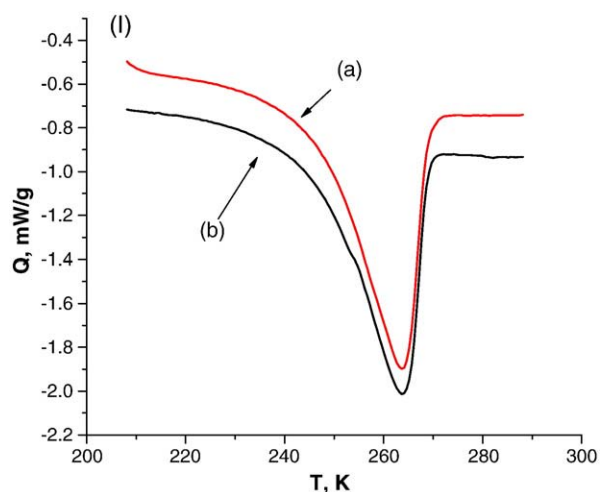


Fig. 5. DSC traces of the samples after isopiestic experiments. (a) Dried powder sample *III* after equilibration in the isopiestic experiment. (b) Gel of SNBD *II* after equilibration in the same isopiestic experiment, initial ratio $M_{H_2O}: M_{ND} = 3.7$.

where $Q_{265\text{ K}}$ denotes the DSC-measured enthalpy that corresponds to the endothermic feature at 265 K.

$V_{H_2O, nm}$ and $V_{H_2O, nm, nf}$ per gram of ND remained almost constant among different gel samples of *II*. Therefore, these two parameters also do not depend on the total amount of water, M_{H_2O} , present in the sample. It was assumed that SNBD is saturated with NPhW as long as bulk water is present [16].

3.2. Isopiestic + DSC

The DSC traces of samples *III* and *II* after equilibration with the vapor of water in the isopiestic experiment are presented in Fig. 5. Only a melting peak of NPhW with the parameters similar to those obtained for the gels was seen in these traces. Dry SNBD powder *III* adsorbed water through the vapor, while SNBD gel *II* lost the bulk water, since the equilibrium vapor pressure in the system was below the saturated vapor pressure of H_2O . Two DSC traces are almost identical. One may conclude that the equilibrium was reached in the system SNBD– H_2O from the two opposite sides.

The temperatures of the broad peaks are almost equal to those measured for the gel samples. It was impossible to measure $\Delta T_m = T_m - T$ in this case. Absolute values of the melting temperature T of NPhW were measured instead. This makes the characteristic diameter D calculated according to Eq. (1) less accurate (see Table 1).

3.3. DSC traces of the gel sample *IIc*

DSC traces of the gel samples prepared from *III* by addition of benzene or heptane are presented in Fig. 6. Broad endothermic

Table 1
Characteristic parameters of samples *II*, *IIa* and *III*, measured by DSC.

Samples	D , nm	$V_{H_2O, nm}$, cm^3/g	$V_{H_2O, nm, nf}$, cm^3/g	$V_{H_2O, nm, nf}$, cm^3/g
SNBD+ H_2O (<i>II</i>)	8.0 ± 1.0	0.48 ± 0.05	0.25 ± 0.05	0.23 ± 0.07
SNBD+ D_2O (<i>IIa</i>)	8.2^a	0.45^a	0.25^a	0.20^a
SNBD+ H_2O (<i>II</i>), isopiestic	7.5 ± 1.2^b	0.43 ± 0.05	0.28 ± 0.05	0.20 ± 0.05
SNBD+ C_6H_6 (<i>III</i>)	7.8 ± 1.2	$0.50^c \pm 0.10$	0.17 ± 0.10^c	0.33 ± 0.10^c
SNBD+ C_7H_{16} (<i>III</i>)	10.8 ± 1.4	$0.50^c \pm 0.10$	0.20 ± 0.10^c	0.30 ± 0.10^c

^a No uncertainty is given since only three independent measurements were taken.

^b The number is based on the measurements of the melting temperature of NPhW. See text for more detail.

^c Volumes of non-bulk, freezing and non-freezing organic solvents, C_6H_6 or C_7H_{16} .

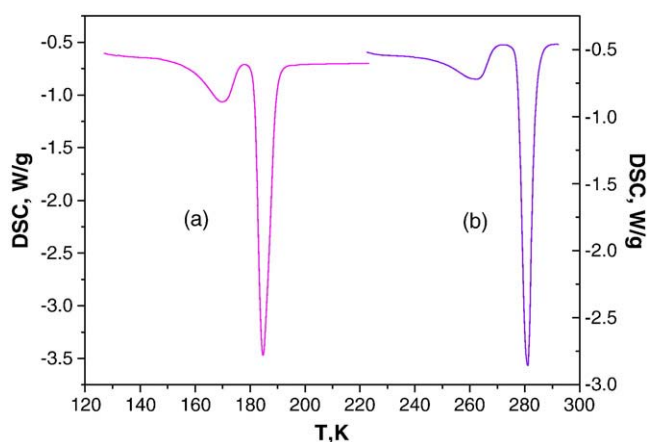


Fig. 6. DSC heating traces of the SNBD gels in organic solvents: (a) sample *III* + C_7H_{16} , (b) sample *III* + C_6H_6 .

features corresponding to the melting of nanophases of organic liquids were found in both traces.

Three parameters of the nanophase were determined using Eqs. (1)–(3) (See Table 1). It is worth noting that SNBD does not form stable liquid dispersions neither with benzene nor with heptane. The surface tensions, $\sigma_{s \rightarrow l}$, of the solid–liquid interfaces for both liquids were taken from literature [24]. These numbers are significantly less accurate than the corresponding surface tension for H_2O [22]. This

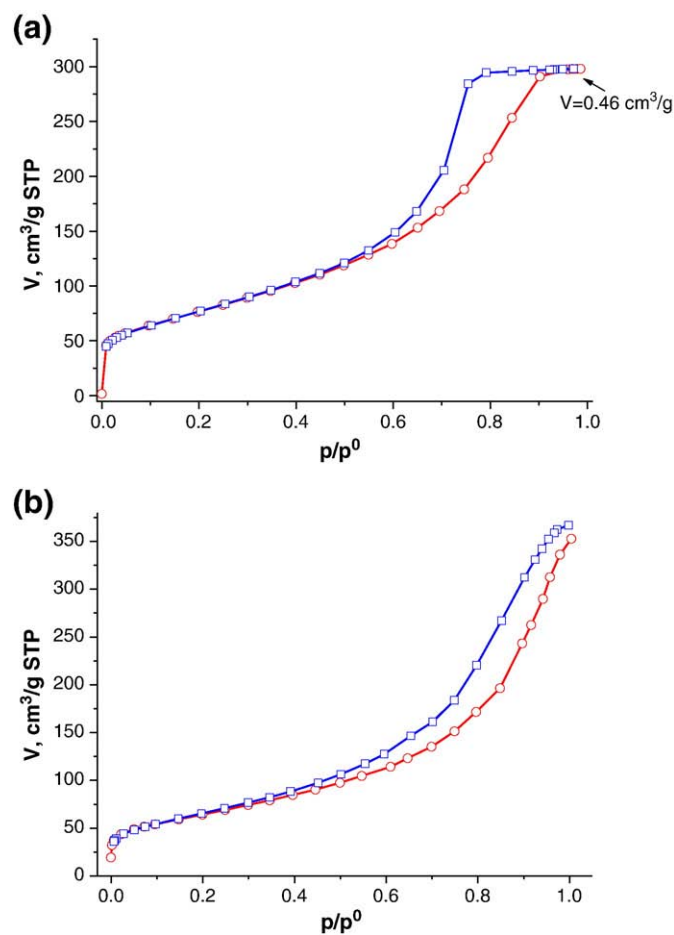


Fig. 7. N_2 adsorption (red)-desorption (blue) isotherms. $T = 77\text{ K}$. a) sample *III*; b) commercial diamond nanoparticles (agglutinates). (For interpretation of the references to color in this figure legend, the reader is referred to the web version of this article.)

makes the uncertainty in the values of the characteristic diameters D to increase significantly (see Table 1). Parameters T_m , ΔH_m , V_L , and ρ for bulk benzene and heptane were taken from a Handbook [27].

3.4. Adsorption of N_2 on SNBD sample III

Typical adsorption–desorption isotherms of N_2 on dried SNBD sample III and on commercial ND material before stirred-media milling are presented in Fig. 7(a,b).

The isotherm in Fig. 7a is of the type IV according to the IUPAC nomenclature [28]. This reveals the presence of the mesopores or voids in the material studied. The standard BJH treatment of the desorption isotherm combines the Gibbs–Kelvin equation for capillary condensation with Harkins–Jura equation for statistical thickness, t_0 , of the adsorbed layer (column 6, Table 2) to give the diameter of the void D' (see Fig. 8). Standard scheme showed a sharp maximum in the void's distribution corresponding to $D' = 9 \pm 1$ nm (column 4, Table 2) which is close to but slightly above the characteristic size D of the NPhW, measured by DSC. The BJH treatment of desorption data for commercial material resulted in broad distribution of voids. Capillary condensation was observed up to the diameters $D' = 30$ nm. The specific surface areas for the sample III and for the commercial samples were almost equal (300 ± 50 m²/g). The total volume of the liquid nitrogen adsorbed by sample III at $p/p^0 \rightarrow 1$ was 0.46 ± 0.05 cm³/g (see Fig. 7a and Table 2).

3.5. Primary particles in the dispersion Ia

Transparent colloidal solution Ia were prepared by re-dispersion of gel II and dried powder III (see Experimental). The results of the DLS measurements are given in Fig. 9. As it is seen from the figure, Ia is a bimodal mixture of small particles ($d < 10$ nm) and of aggregates ($d \sim 80$ nm). Most of the scattering occurs on aggregates (89% of intensity), however small particles dominate in number distribution of particle population (almost 100%). The composition of the aqueous colloid Ia is similar to those of colloid I. [11]. The DLS measurements were taken over a period of 7 days and no change in composition was observed.

A drop of the aqueous colloid Ia was spread over the glass and water was quickly removed from the sample. TEM picture of the dry residual is given in Fig. 10.

TEM confirms the presence of small ($d < 10$ nm) particles in the dispersed sample (Fig. 10a).

Aggregates however were also detected. In the TEM picture (Fig. 10b) irregular internal system of voids could be seen.

4. Discussion

The experimental results are summarized in Tables 1 and 2.

Table 2
Characteristics of the SNBD material.

Experimental method	Samples	D , nm	$D' = D + 2t_0$, nm	V_{nm} , cm ³ /g ND	t_0 , nm
DSC, water	II, IIIa	8.0 ± 1.0	$< 10.0^{a,b}$	0.48 ± 0.05	$< 1.0^b$
DSC+isopiestic	III, IIIa	7.5 ± 1.2		0.43 ± 0.10	
N_2 adsorption	III	7.0^a	9 ± 1	0.46 ± 0.05	1.0^c
DSC, organic liquids:	IIb	7.8 ± 1.2	$< 10.4^{a,b}$	0.50 ± 0.10	$< 1.3^b$
C_6H_6 C_7H_{16}		10.8 ± 1.4	$< 12.6^{a,b}$	0.50 ± 0.10	$< 0.9^b$

^a Estimated by using Eq. (4).

^b Upper limit, calculated under the assumption that the whole amount of non-freezing liquids forms the surface layer inside the voids.

^c Statistical thickness, t_0 , calculated by Harkins–Jura equation.

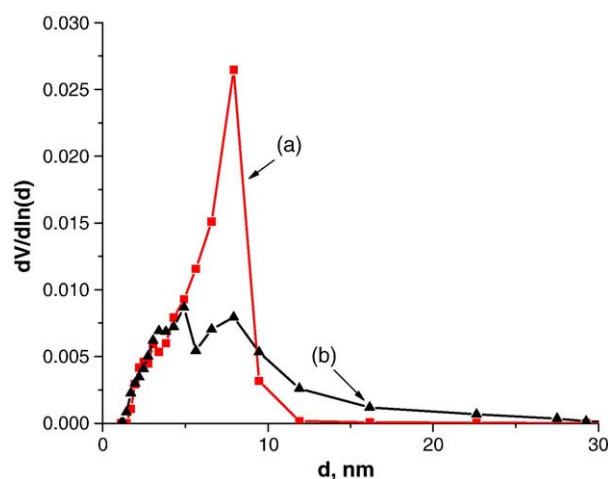


Fig. 8. BJH analysis of the desorption isotherms. a) sample III; b) commercial diamond nanoparticles (agglutinates).

4.1. NPhW, organic nano-liquids and voids

The data obtained with DSC basically refer to the properties of NPhW, therefore it is necessary to find a proper place for NPhW within the system. NPhW demonstrated two different size-effects, namely depression of the melting point (gel by DSC) and capillary condensation (dried powder by isopiestic experiment). In order for this to happen the meniscus must be concave for the liquid NPhW at the gas–liquid and solid–liquid interfaces as shown in Fig. 11. This is possible if NPhW is mostly placed in between the ND particles. From this we conclude that NPhW in the gel phase and the dried powder is confined to the voids within the network, formed by SNBD particles. These voids were assumed to be cylindrical which is a commonly used approximation. Capillary condensation of nitrogen occurred into the same voids. Under this assumption, we can write:

$$D = D' - 2t_0 \quad (4)$$

where thickness t_0 refers to surface layer of adsorbed nitrogen, water or organic liquids. Using Eq. (4) we can compare the diameters D and D' , obtained from DSC and adsorption measurements, respectively (Table 2, columns 3 and 4). Characteristic diameters D and D' and total volumes of NPhW and of adsorbed nitrogen calculated from DSC and

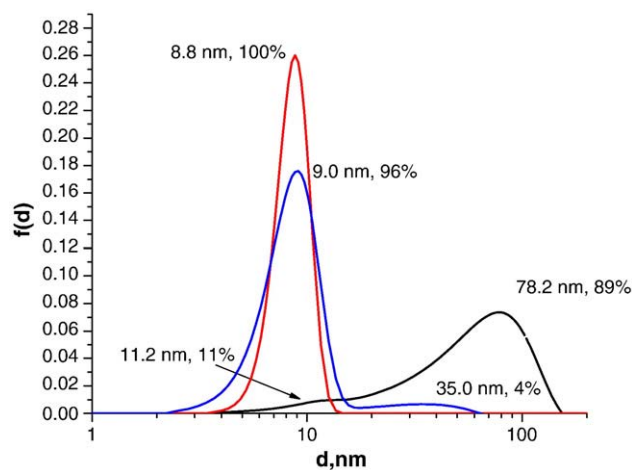


Fig. 9. Distribution of particles in the water dispersion Ia after 25 min of sonication (80 W). Black line – distribution by intensity; Red line – distribution by number of particles; Blue line – distribution by volume. (For interpretation of the references to color in this figure legend, the reader is referred to the web version of this article.)

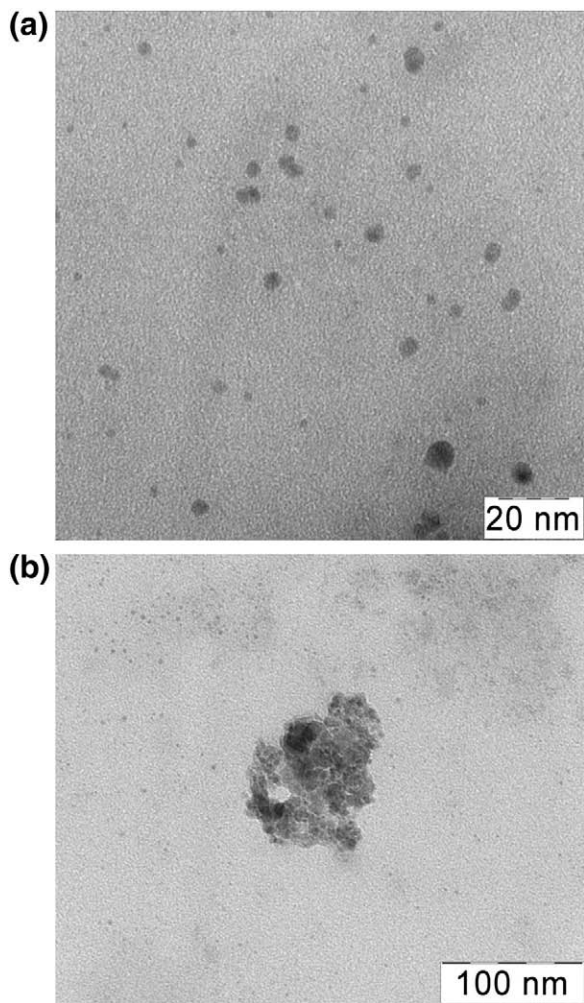


Fig. 10. TEM images of the sample, prepared by drying of Ia on glass. a) primary particles and small clusters b) aggregate with visible porous structure.

adsorption data are all close (Table 2). DSC data for two organic liquids gave additional confirmation of this approach. Non-freezing part of NPhW is in direct contact with the surfaces of SNBD particles. The thickness of the layer, t_0 , can be calculated from $V_{H_2O, nm, nf}$

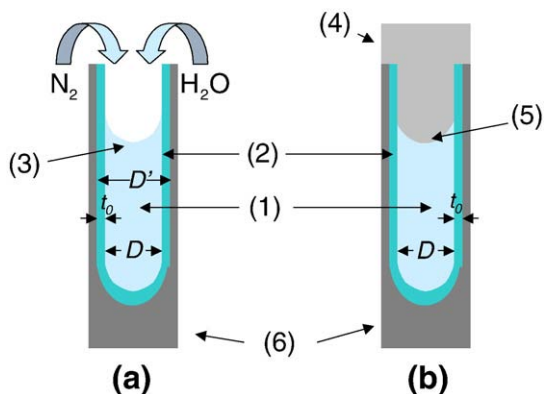


Fig. 11. Sketch of the cylindrical void. (a) Isoopiestic experiment and adsorption of nitrogen, (b) melting of NPhW. (1) liquid NPhW (a,b) or liquid nitrogen (a), D = characteristic diameter of NPhW measured by DSC, D' = characteristic diameter of void calculated from adsorption and DSC data; (2) non-freezing NPhW (a,b) or adsorbed nitrogen (a), t_0 = thickness of the layer; (3) concave meniscus of the NPhW or nitrogen on the interface gas-liquid; (4) bulk ice; (5) concave meniscus of the NPhW on the interface solid-liquid; and (6) SNBD.

obtained for H_2O by DSC. The same calculations can be performed for organic solvents. For N_2 the thickness t_0 was calculated with the Harkins–Jura equation. In all cases the thickness corresponds to 2–4 monolayers, which is typical [22–24].

In order to confine NPhW it seems reasonable to consider non-cylindrical voids within the close-packed structure formed by primary ND. This assumption, however, is inconsistent with the results of adsorption measurements. It was shown that for all types of the close packing, characteristic effective diameter D' calculated from adsorption data must be 1.3–4 times smaller than the diameter d of the spherical particles, which form the structure [29]. In our case D (7–8 nm) and D' (9–10 nm) are even larger than the diameter of the SNBD particles (5.2 nm, [12]). One may conclude that the most part of nitrogen and of the freezing NPhW occupies the larger voids than those existed within the close-packed arrangements. Formation of such voids was confirmed in the present study by four types of independent measurements.

The voids with D (7–8 nm) and D' (9–10 nm) fit the network formed by nonporous ND aggregates with $d = 15–40$ nm. If to assume such network to exist, one has to observe stable and sharp distribution of aggregates with $d = 15–40$ nm by DLS or TEM. We never saw the aggregates of such size in this study. Aggregates with $d = 78$ nm (see Fig. 9) are too big to form a network with D (7–8 nm) and D' (9–10 nm).

4.2. Secondary structure of SNBD

The results obtained above revealed that gel and dried powder of SNBD material exist in structures rather than in chaotic and weakly bonded mixtures of the individual particles. The size and the total number of voids characterized these structures. They were observed by conventional methods based on Gibbs–Thomson equation and capable of detecting mesopores (voids). No direct confirmation came from microscopy.

Strong cohesive interaction between neighboring carbon nanoparticles (e.g. fullerenes in polar solvents [30], carbon nanotubes [31] and nanohorns [32], ND particles with the sharp size distribution [33]), caused by large surface area to volume ratios is a well-known fact. The perfectly dispersed state of SNBD particles is likely to happen only in colloidal solution. Some sort of self-assembly is bound to occur in gels and dry powders where individual primary SNBD particles are put close to each other, thus forming a network. Independence of the parameters measured from the way of disintegration of agglutinates and preparation of sample II, III proves the stability of the network. It is worth noting that addition of water, which causes transition from the dried powder to the gel state of SNBD material, did not increase the size of the voids, while mild pressing of the dry powders prior to the addition of water did not decrease it. One and the same surprisingly reproducible results were obtained when sample II were converted into sample III and back. It was assumed that the stable ND network is formed already in the gel state and is the same for the dry powders. The network is at least partially re-dispersible into the aqueous colloid solution of primary particles by means of mild ultrasonication i.e. sample I could be converted into sample II and back. This proves that primary particles are the most likely building blocks of the network.

The voids account for approximately 63% of the total volume of the structure. If one considers the freezing part of NPhW only, this number goes down to 46%. It is possible to make both numbers smaller (57 and 41%, respectively), if one assumes that the density of a SNBD particle, ρ , is smaller than the density of bulk diamond and is equal to 2.87 g/cm³ due to the presence of the sp² shell around each primary ND [34]. The experimental methods used in this study do not provide any information about distribution of the voids within the SNBD.

The reproducible aggregation network observed could be compared with the unique structure formed by carbon nanohorns [32]. The nanohorns ensured intimate mating of the bonding surfaces with

$D' \approx 1$ nm as measured by N_2 adsorption. For SNBD the size of voids (D or D') is larger than the diameter of the primary particles. Such large pieces of empty space within the network make one to think about the repulsing forces preventing primary particles from occupying of this space.

The authors [8,9] predicted interfacial Coulombic interaction between neighboring primary SNBD particles. In Refs. [8,9] primary particles were considered to be nanocrystals with different surface electrostatic potential at different facets. It is worth noting, that the arrangements predicted in Ref. [9] include voids of the size, larger than the size of primary SNBD particles (Fig. 3 in Ref. [9]). Similar monolayered structure with visible voids formed by Fe_3O_4 nanoparticles ($d = 12$ – 14 nm) was observed in [35]. According to the authors of Ref. [35] “the orientation ordered superlattices” were formed due to the Van der Waals interactions.

5. Conclusion

In the present work we introduced a porous network structure for assembled forms of particles in gel and dried powder of SNBD material. We found that in gel and dried powder the primary SNBD particles form one and the same reproducible porous network with voids larger than the SNBD itself. These facts taken together are rather surprising. Three characteristic parameters of the hydration process (D , $V_{H_2O, nm}$ and $V_{H_2O, nm, f}$) are well retained, hence we consider them as fingerprints of SNBD material. The volume of the voids may range from 47 to 63% of the total volume of SNBD. This free volume is readily available for water, some organic solvent molecules, nitrogen at low temperatures, and even larger molecules like drugs. Further work will be necessary to elucidate the nature of underlying forces that maintain the mesoporous network. The results obtained in this work showed that individual primary SNBD particles could be dispersed only in sufficiently dilute colloidal solutions. Removal of solvent medium leads to spontaneous self-assembly. This latter process, as long as it is reversible, does not impair the properties of SNBD. The voids found in the SNBD network structures could accommodate foreign molecules, which makes them promising candidate for the drug delivery and probably for many other applications.

Acknowledgements

M.K., M.B., N.A. and N.I. are supported by the RFBR grant 09-03-00004. M.K. and M.B. are also supported by the grant for Leading Scientific Schools in Russia 428.2008.3. Authors are grateful to Dr. E.

Knyazeva for her help in arranging of the adsorption measurements and to A. Gagarin for his participation in the isopiestic experiments.

References

- [1] E. Osawa, Pure Appl. Chem. 80 (7) (2008) 1365.
- [2] V. Dolmatov, Uspechi khimii 76 (4) (2007) 375 in Russian.
- [3] O. Shenderova, V. Zhirnov, D. Brenner, Critical Reviews in Solid State and Materials Sciences 27 (2002) 227.
- [4] A. Krueger, Chemistry European journal 14 (2008) 1382.
- [5] P. Nesterenko, O. Fedyanina, Yu. Volgin, Analyst 132 (5) (2007) 403.
- [6] T. Huang, Y. Zeng, Y. Liu, Y. Chen, K. Walker, R. Guntupalli, C. Liu, Diamond and related materials 13 (4–8) (2004) 1098.
- [7] S. Yu, M. Kang, H. Chang, K. Chen, Y. Yu, JACS 127 (2005) 17604.
- [8] A. Barnard, M. Sternberg, J. Mater. Chem. 17 (2007) 4811.
- [9] A. Barnard, J. Mater. Chem. 18 (2008) 4038.
- [10] S. Osswald, G. Yushin, V. Mochalin, S. Kucheyev, Yu. Gogotsi, JACS 128 (35) (2006) 11635.
- [11] A. Kruger, F. Kataoka, M. Ozawa, A. Aksenskii, A. Vul', Y. Fjino, A. Suzuki, E. Ōsawa, Carbon 43 (8) (2005) 1722.
- [12] M. Osawa, M. Inaguma, T. Takahashi, F. Kataoka, A. Kruger, E. Osawa, Advanced Materials 19 (2007) 1201.
- [13] I. Kulakova, Russian Chemical Journal 48 (2004) 97.
- [14] Fedutik Yu, A. Antipov, E. Maltseva, A. Kalchev, T. Gubarevich. Non-aggregated detonation nanodiamonds. Proceedings of 3rd International Symposium «Detonation Nanodiamonds: Technology, Properties and Applications», St. Petersburg, Russia, 2008, p. 65.
- [15] X. Fang, J. Mao, E. Levin, JACS 131 (4) (2008) 1426.
- [16] M. Korobov, N. Avramenko, A. Bogachev, N. Rozhkova, E. Ōsawa, J. Phys. Chem. C 111 (20) (2007) 7330.
- [17] K. Iakoubovskii, K. Mitsuishi, K. Furuya, Nanotechnology 19 (2008) 1.
- [18] H. Huang, E. Pierstorff, E. Osawa, D. Ho, Nano Letters 7 (11) (2007) 3305.
- [19] R. Lam, M. Chen, E. Pierstorff, H. Huang, E. Ōsawa, D. Ho, ACS Nano 2 (10) (2008) 2095.
- [20] H. Huang, E. Pierstorff, E. Osawa, D. Ho, ACS Nano 2 (2) (2008) 203.
- [21] C. Faivre, D. Bellet, G. Dolino, The European Physical Journal B 7 (1999) 19.
- [22] K. Ishikiriya, M. Todoki, K. Motomura, J. Colloid Interface Sci. 171 (1995) 92.
- [23] H. Christenson, Journal of Physics: Condensed Matter 13 (2001) R95.
- [24] C. Jackson, G. McKenna, J. Chem. Phys. 93 (12) (1990) 9002.
- [25] M. Plooster, S. Gitlin, J. Phys. Chem. 75 (21) (1971) 3322.
- [26] M. Korobov, E. Stukalin, N. Ivanova, N. Avramenko, G. Andrievsky, in: P. Kamat, D. Guldi, K. Kadish (Eds.), The Exciting World of Nanocages and Nanotubes, vol 12, Electrochemical Society, Pennington NJ, 2002, p. 799.
- [27] CRC Handbook of Chemistry and Physics 77th ed, CRC Press, Boca Raton, FL, 1996.
- [28] K. Sing, D. Everett, R. Haul, L. Moscou, R. Pierotti, J. Rouquerol, T. Siemieniowska, Pure Appl. Chem. 57 (1985) 603.
- [29] A. Karnauchov, A. Kiselev, Russian Journal of Physical Chemistry 31 (12) (1957) 2635.
- [30] R. Alargova, S. Deguchi, K. Tsujii, JACS 123 (2001) 10460.
- [31] A. Sadans, A. Peera, J. Chattopadhyay, Z. Gu, R. Hauge, W. Billups, Nano Lett. 4 (7) (2004) 1257.
- [32] E. Bekyarova, A. Hashimoto, M. Yudasaka, Y. Hattori, K. Murata, H. Kanoh, D. Kasuya, S. Iijima, K. Kaneko, J. Phys. Chem. B 109 (9) (2005) 3711.
- [33] V. Grichko, T. Tyler, V.I. Grishko, O. Shredova. Nanodiamond particles forming photonic structures. Nanotechnology 2008, 19: 225201 (5pp).
- [34] M. Avdeev, N. Rozhkova, V. Aksenov, V. Garamus, R. Willumeit, E. Osawa, J. Phys. Chem. C 113 (2009) 9473.
- [35] Q. Song, Y. Ding, Z.L. Wang, Z. Zhang, J. Phys. Chem. B 110 (2006) 25547.